



Transient HES5 Activity Instructs Mesodermal Cells toward a Cardiac Fate

Ana G. Freire,^{1,2,3,4,12} Avinash Waghray,^{3,5} Francisca Soares-da-Silva,^{1,2,6,7} Tatiana P. Resende,^{1,2}

Dung-Fang Lee,^{3,8} Carlos-Filipe Pereira,^{3,9} Diana S. Nascimento,^{1,2} Ihor R. Lemischka,^{3,10,11}

and Perpétua Pinto-do-Ó^{1,2,7,11,*}

¹i3S – Instituto de Investigação e Inovação em Saúde

²INEB – Instituto de Engenharia Biomédica

Universidade do Porto, 4200-135 Porto, Portugal

³Department of Cell, Developmental and Regenerative Biology and The Black Family Stem Cell Institute, Icahn School of Medicine at Mount Sinai, New York, NY 10029, USA

⁴Faculdade de Engenharia, Universidade do Porto, 4200-465 Porto, Portugal

⁵Graduate School, Icahn School of Medicine at Mount Sinai, New York, NY 10029, USA

⁶Faculdade de Medicina, Universidade de Coimbra, 3004-504 Coimbra, Portugal

⁷Instituto de Ciências Biomédicas Abel Salazar, Universidade do Porto, 4050-313 Porto, Portugal

⁸Department of Integrative Biology and Pharmacology, McGovern Medical School, The University of Texas Health Science Center at Houston, Houston, TX 77030, USA

⁹CNC, Center for Neuroscience and Cell Biology, University of Coimbra, 3060-197 Cantanhede, Portugal

¹⁰Department of Pharmacological Sciences, Icahn School of Medicine at Mount Sinai, New York, NY 10029, USA

¹¹Co-senior author

¹²Present address: Division of Regenerative Medicine, Department of Medicine, Ansary Stem Cell Institute, Weill Cornell Medical College, New York, NY 10065, USA

*Correspondence: perpetua@ineb.up.pt

<http://dx.doi.org/10.1016/j.stemcr.2017.05.025>

SUMMARY

Notch signaling plays a role in specifying a cardiac fate but the downstream effectors remain unknown. In this study we implicate the Notch downstream effector HES5 in cardiogenesis. We show transient *Hes5* expression in early mesoderm of gastrulating embryos and demonstrate, by loss and gain-of-function experiments in mouse embryonic stem cells, that HES5 favors cardiac over primitive erythroid fate. *Hes5* overexpression promotes upregulation of the cardiac gene *Isl1*, while the hematopoietic regulator *Sc1* is downregulated. Moreover, whereas a pulse of *Hes5* instructs cardiac commitment, sustained expression after lineage specification impairs progression of differentiation to contracting cardiomyocytes. These findings establish a role for HES5 in cardiogenesis and provide insights into the early cardiac molecular network.

INTRODUCTION

During embryogenesis, cardiac precursors derive from mesodermal cells that ingress through the primitive streak and segregate shortly after migration of prospective hematopoietic progenitors to the yolk sac (Parameswaran and Tam, 1995). Signaling pathways governing heart formation are often functional or reactivated in cardiac disease, such as the example of Notch, whose activation after myocardial infarction has been correlated with repair and pro-survival processes (reviewed in Freire et al., 2014). Thus, understanding the mechanisms underlying cardiac fate is essential in envisaging new strategies for improved cardiac repair/regeneration.

Notch signaling is crucial for heart formation, and loss-of-function mutations in several pathway components result in severe cardiac phenotypes, including impaired trabeculation and ventricular septal defects (reviewed in Nemir and Pedrazzini, 2008). Notch signaling is mediated by the interaction of transmembrane receptors (NOTCH1–4) and ligands (JAGGED1 and 2 and DLL1, 3, and 4) expressed on the surface of neighboring cells. Ligand-receptor binding results in the release of the Notch

intracellular domain (NICD) which translocates to the nucleus and binds RBP-Jk/CSL, activating transcription of Notch downstream targets. These include members of *Hes* and *Hes-related* (also known as *Hey*) gene families encoding basic helix-loop-helix (bHLH) transcription factors that mediate important Notch functions, such as maintenance of progenitors and binary cell fate decisions (reviewed in High and Epstein, 2008; Kageyama et al., 2007).

The effects of Notch are dependent on the cellular context and timing of the signal. For example, transient Notch activation in mouse embryonic stem cell (mESC)-derived hemangioblasts redirects differentiation to a cardiac fate, suggesting a role in specifying the cardiac lineage (Chen et al., 2008). Likewise, NICD1 expression in nascent mesodermal cells in the embryo (Del Monte et al., 2007) supports a role in mesodermal patterning at the time cardiac progenitors are specified. However, activation of Notch in the early *Xenopus* heart field (Rones et al., 2000) and in murine cardiogenic mesoderm (Watanabe et al., 2006) suppresses myocardial differentiation.

We aimed to identify NICD1 targets playing a role at the onset of cardiogenesis. We show that *Hes5* is expressed in gastrulating mesoderm and instructs cardiac over primitive

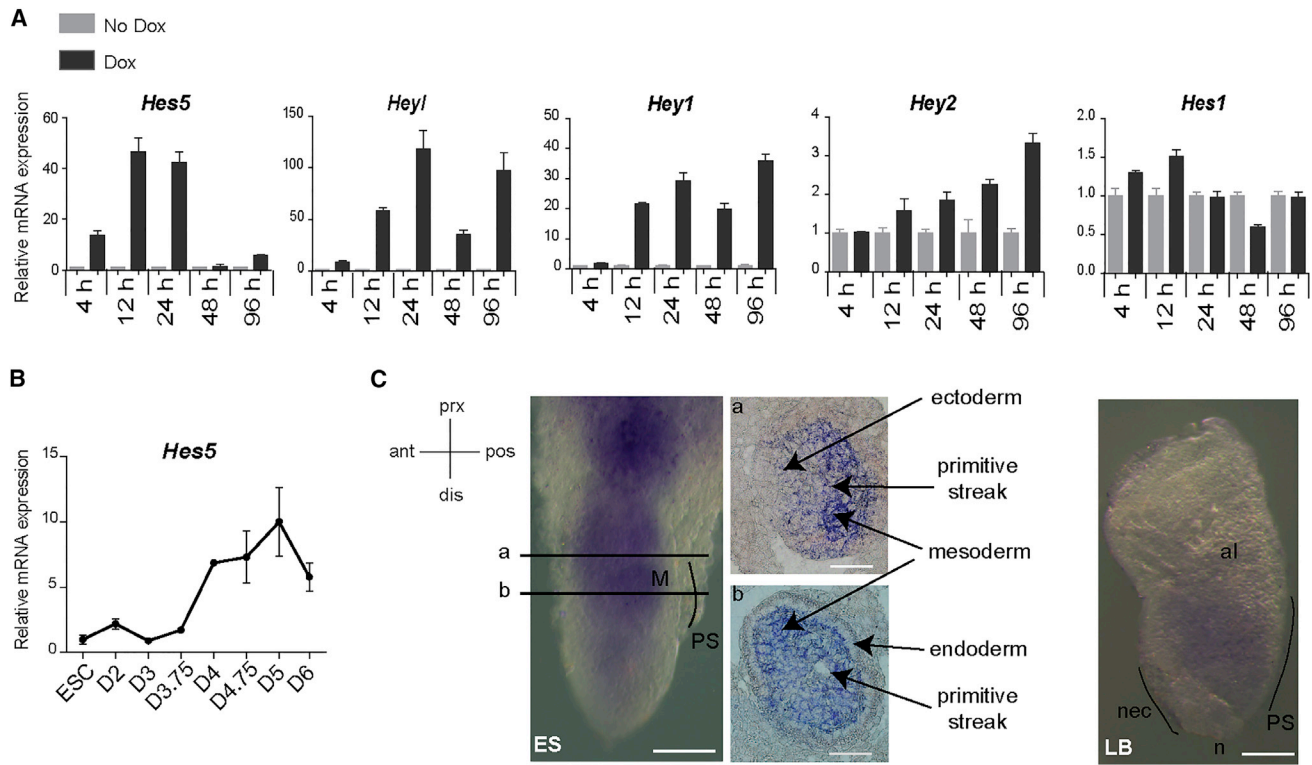


Figure 1. Expression of the NICD1 Target *Hes5* during mESC Differentiation and in Mouse Embryos

(A) Real-time qPCR analysis of *Hes5*, *Heyl*, *Hey1*, *Hey2*, and *Hes1* after NICD1 activation in Bry-GFP⁺ cells shows a peak upregulation of *Hes5*. (B) *Hes5* expression profile during mESC differentiation to mesodermal derivatives. Error bars represent mean \pm SEM of three experiments. D, day.

(C) Whole-mount *in situ* hybridization for *Hes5* in early-streak (ES) and late-bud (LB) embryos (scale bars, 100 μ m). Transversal sections at the indicated positions (a and b; scale bars, 50 μ m). ant, anterior; pos, posterior; prx, proximal; dis, distal; M, mesoderm; PS, primitive streak; al, alantoid; n, node; nec, neuroectoderm.

See also Figure S1.

erythroid fate in mESC-derived mesodermal progenitors, while regulating important cardiac and hematopoietic genes such as *Isl1* and *Scl*. Moreover, after cardiac induction, *Hes5* withdrawal is required to allow differentiation to contracting cardiomyocytes. Our results establish a context- and time-dependent role for HES5 in cardiogenesis.

RESULTS

Hes5 Expression during mESC Differentiation and in Gastrulating Embryos Suggests a Role in Mesodermal Patterning Downstream of NICD1

To identify NICD1 targets involved in cardiac specification, we used AinV/Bry-GFP/NICD1 mESCs (Cheng et al., 2008) that express NICD1 under the control of a doxycycline (Dox)-inducible promoter and harbor GFP targeted to the *Brachyury* locus (Bry-GFP), a pan-meso-

dermal marker. We analyzed the expression of the Notch targets *Hes5*, *Heyl*, *Hey1*, *Hey2* and *Hes1*, at 4, 12, 24, 48, and 96 hr after activating NICD1 in Bry-GFP⁺ mesodermal cells. *Hes5*, *Heyl*, and *Hey1* were upregulated, while *Hey2* was only increased at later time points and *Hes1* was not altered (Figure 1A). *Hes5* levels were highly increased up to 24 hr followed by a dramatic decrease, suggesting a time-dependent regulation. We then analyzed the expression profile of *Hes5* during mESC differentiation to mesodermal derivatives in the absence of NICD1 activation. *Hes5* levels increased from day 3.75 (D3.75) to D5, and decreased at D6 (Figure 1B). The timing of *Hes5* upregulation corresponds to the temporal window in which mesoderm is specified to its derivatives, as demonstrated by the expression profile of mesodermal and early cardiac and hematopoietic regulators (Figure S1A). *Hes5* expression was also analyzed in early development by whole-mount *in situ* hybridization in mouse embryos from embryonic day 6.5 (E6.5) to E9.5. *Hes5* transcripts were detected in

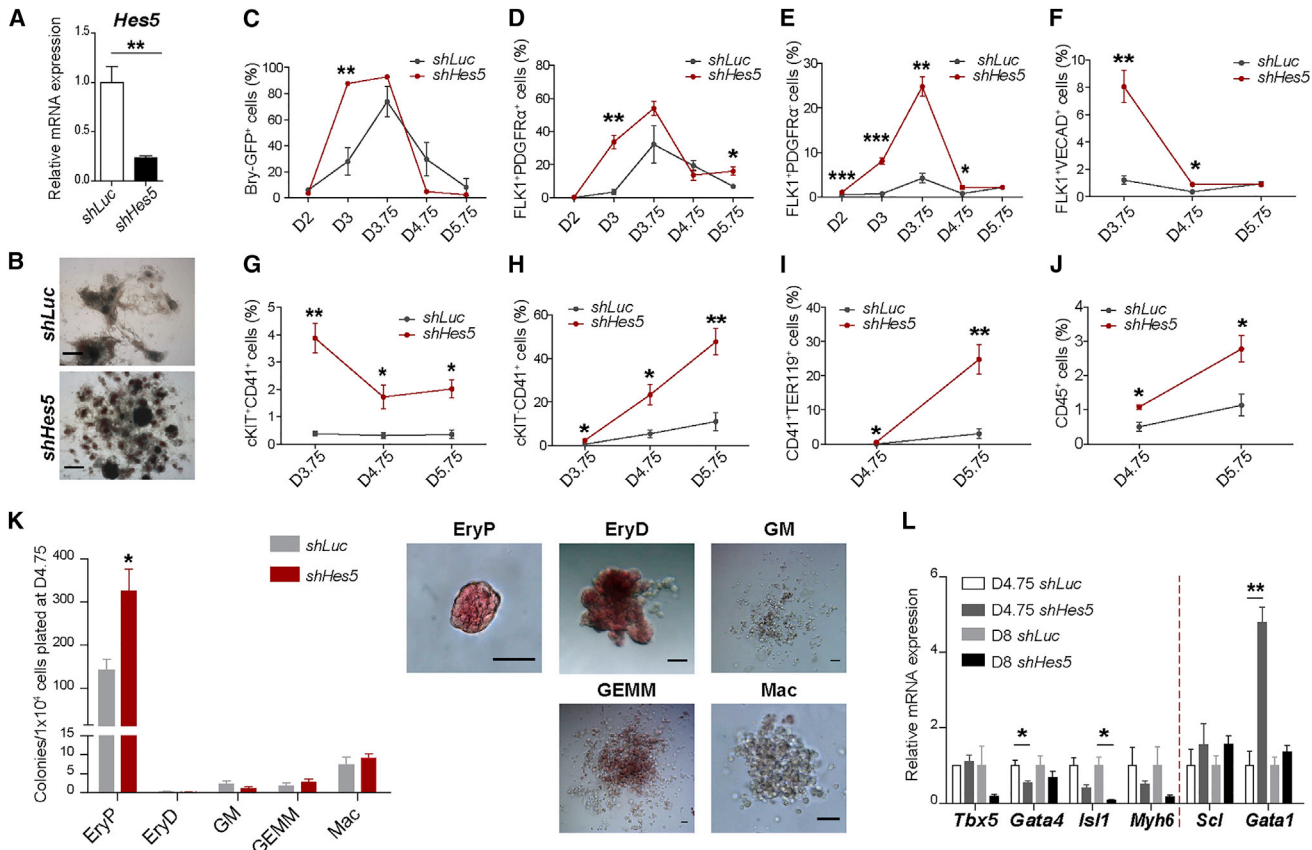


Figure 2. Enhanced Primitive Erythropoiesis in Hes5-KD mESCs

(A) *Hes5* expression in cells transduced with *shLuc* or *shHes5*.

(B) Morphological evaluation of *shLuc*- or *shHes5*-transduced cells. Scale bars, 200 μ m.

(C–J) Percentage of cells analyzed by flow cytometry expressing mesodermal (Bry-GFP, FLK1, and PDGFR α), endothelial (VECAD), and hematopoietic (cKIT, CD41, TER119, CD45) markers in *shLuc*- and *shHes5*-transduced cells from day 2 (D2) to D5.75.

(K) Quantification and images of representative hematopoietic colonies of EryP (primitive erythroid), EryD (definitive erythroid), GM (granulocyte-macrophage), GEMM (granulocyte-erythrocyte-megakaryocyte-macrophage), and Mac (macrophage). Scale bars, 50 μ m.

(L) Real-time qPCR data for cardiac (*Tbx5*, *Gata4*, *Isl1*, *Myh6*) and hematopoietic (*Scl*, *Gata1*) genes in *shLuc*- and *shHes5*-transduced cells at D4.75 and D8.

Error bars represent mean \pm SEM of three (or five in K) experiments. *p < 0.05, **p < 0.01, ***p < 0.001. See also Movies S1 and S2.

nascent mesodermal cells of early-streak (ES, n = 6/7) and mid-streak (MS, n = 4/4) embryos (Figures 1C and S1B). At this early stage, epiblast cells ingressing through the primitive streak are fated to become extraembryonic mesoderm and cranial-cardiac mesoderm (Parameswaran and Tam, 1995). *Hes5* was not expressed (n = 5/8) or was dramatically downregulated (n = 3/8) in late-bud (LB) stage embryos (Figures 1C and S1B). Embryos at later stages exhibited *Hes5* in ectoderm and neuronal structures as expected (Figure S1B). The transient *Hes5* expression in gastrulating mesoderm and during mesodermal differentiation in mESCs suggests a time-specific role during early mesodermal specification to cardiac and hemogenic lineages.

Depletion of *Hes5* Enhances Primitive Erythropoiesis in mESCs

We asked whether HES5 is a mediator of NICD1 in the specification of a cardiac fate. A fine dissection of early events during embryonic development is technically challenging when using mouse embryos, particularly in the case of a transient expression profile. Hence, we pursued our studies profiting of the robustness of the mESC differentiation system in replicating the early embryo development (reviewed in Murry and Keller, 2008). For *Hes5* depletion, cells were transduced with a short hairpin RNA (shRNA) (*shHes5*) or a control shRNA targeting Luciferase (*shLuc*) (Figure 2A). Interestingly, in *Hes5*-knockdown (KD) cultures hematopoietic-like cells were predominant, and



only rare contracting areas emerged (Figure 2B and Movie S1). In contrast, control cultures presented cardiomyocytes and hematopoietic cells (Figure 2B and Movie S2).

In the developing vertebrate embryo, the first wave of hematopoiesis occurs in the yolk sac and contributes principally primitive erythroid cells (reviewed in Tavian and Peault, 2005). To investigate the role of HES5 in the emergence of the hematopoietic lineage, we carried out a time-course flow-cytometry analysis from D2 to D5.75 of *in vitro* differentiation following *Hes5*-KD. Primitive mesodermal progenitors co-express FLK1 and platelet-derived growth factor receptor α (PDGFR α), whereas in vascular/hematopoietic mesoderm PDGFR α expression is downregulated (Kataoka et al., 2011). The kinetics of Bry-GFP $^+$ and FLK1 $^+$ PDGFR α $^+$ mesodermal cells was similar to that of the control with highest frequency reached at D3.75, although the percentage was increased at D3 and also at D5.75 in the FLK1 $^+$ PDGFR α $^+$ population (Figures 2C and 2D). Importantly, the frequency of FLK1 $^+$ PDGFR α $^-$ hemogenic progenitors was significantly enhanced after *Hes5* downregulation (up to 10.2-fold) (Figure 2E). Favored hemogenic commitment in *Hes5*-KD cells was also supported by a significant increase in the percentage of FLK1 $^+$ VE-CADHERIN $^+$ cells (FLK1 $^+$ VECAD $^+$, Figure 2F) and in cKIT $^+$ CD41 $^+$ hematopoietic progenitors (Figure 2G) (up to 6.7- and 10.1-fold, respectively). *Hes5*-KD cultures contained higher numbers of cKIT $^-$ CD41 $^+$ differentiated hematopoietic cells (Figure 2H), particularly CD41 $^+$ TER119 $^+$ early erythroid precursors (Figure 2I) (up to 4.3- and 12.9-fold increase, respectively). In addition, a higher percentage of cells expressing the pan-hematopoietic marker CD45 was observed in *Hes5*-KD cultures (up to 2.5-fold increase) (Figure 2J). To confirm that depletion of *Hes5* promoted hematopoiesis, we performed colony-forming unit (CFU) assays. No colonies emerged in both control and *Hes5*-KD cultures from cells plated in methylcellulose-based medium at D3.75 (not shown). *Hes5*-KD cells plated at D4.75 created a significantly higher number of primitive erythroid (EryP) colonies (2.3-fold) (Figure 2K), consistent with the increased frequency of erythroid progenitors emerging earlier during differentiation. We did not observe an effect on the differentiation to other hematopoietic lineages (Figure 2L). These results suggest that loss of *Hes5* in mESCs favors the emergence of the first wave of hematopoiesis, which primarily contributes EryP.

Following these observations, expression of cardiac genes (*Tbx5*, *Gata4*, *Isl1*, and *Myh6*) and hematopoietic regulators (*Scl* and *Gata1*) was analyzed. Cardiac genes were downregulated in *Hes5*-KD cells (varying from 2.0-fold up to 12.5-fold), especially *Gata4* at D4.75 and *Isl1* at D8 of differentiation; *Scl* expression was similar to control at these stages and the erythroid master regulator *Gata1* was signif-

icantly upregulated at D4.75 (4.8-fold) and comparable with the control at D8 (Figure 2L).

Altogether these data demonstrate that loss of *Hes5* in mESCs enhances primitive erythropoiesis, and support a role in the regulation of cardiac versus primitive erythroid fate in early mesodermal progenitors.

HES5 Instructs Cardiac Over Primitive Erythroid Differentiation in mESC-Derived Mesodermal Cells

To better understand the role of HES5 in the specification of mesodermal lineages, we used a Dox-inducible gain-of-function system to express exogenous FLAG-tagged *Hes5* (Figure 3A) in reverse tetracycline transactivator (rtTA)-expressing AinV/Bry-GFP mESCs. Given the context-dependent role of HES factors, we induced pulses of *Hes5* at distinct stages of differentiation (D2–D3, D3–D3.75, D3.75–D4.75, and D4.75–D5.75) and quantified the number of contracting foci. Interestingly, only activation at D3.75 significantly promoted the emergence of contracting foci (from 3.4-fold up to 5.0-fold increase) (Figure 3B; Movies S3 and S4), correlating with the results on the endogenous *Hes5* levels (Figure 1B). Next, we investigated the effect of *Hes5* induction at D3.75 on hematopoietic differentiation. After 48 hr of Dox treatment, the number of cKIT $^+$ CD41 $^+$ and cKIT $^-$ CD41 $^+$ cells was decreased (1.9- and 2.1-fold, respectively) (Figures 3C and 3D). Importantly, *Hes5* overexpression led to a dramatic reduction in CD41 $^+$ TER119 $^+$ early erythroid precursors (10.4-fold) (Figures 3C and 3D) and *Gata1* downregulation (4.2-fold) (Figure 3E). Moreover, cells induced at D3.75 and subjected to CFU assays at D4.75 or at D5.75 created a lower number of EryP colonies (2.1- and 2.8-fold, respectively) (Figure 3F), corroborating the effect on primitive erythropoiesis observed in *Hes5*-KD cells. Both time points showed similar potential of differentiation to other hematopoietic lineages that was not altered after *Hes5* induction (Figure 3F).

Next, we addressed whether preferential cardiac fate results from a selective or instructive action in primitive mesodermal cells. Proliferation and apoptosis were analyzed after *Hes5* activation in Bry-GFP $^+$ FLK1 $^+$ PDGFR α $^+$ cells isolated at D3.75. The results indicate that HES5 does not promote the selection of particular subsets of progenitors, as non-induced and induced cultures contained a similar percentage of proliferative (Figure 3G) and apoptotic cells (Figure 3H) after 24 and 36 hr, respectively. Together our data demonstrate a time-specific and instructive role for HES5 in specifying early mesodermal cells to a cardiac over a primitive erythroid fate.

HES5 Regulates Cardiac and Hematopoietic Genes in Mesodermal Cells Including *Isl1* and *Scl*

HES proteins regulate transcription by DNA binding-dependent and -independent mechanisms; the latter

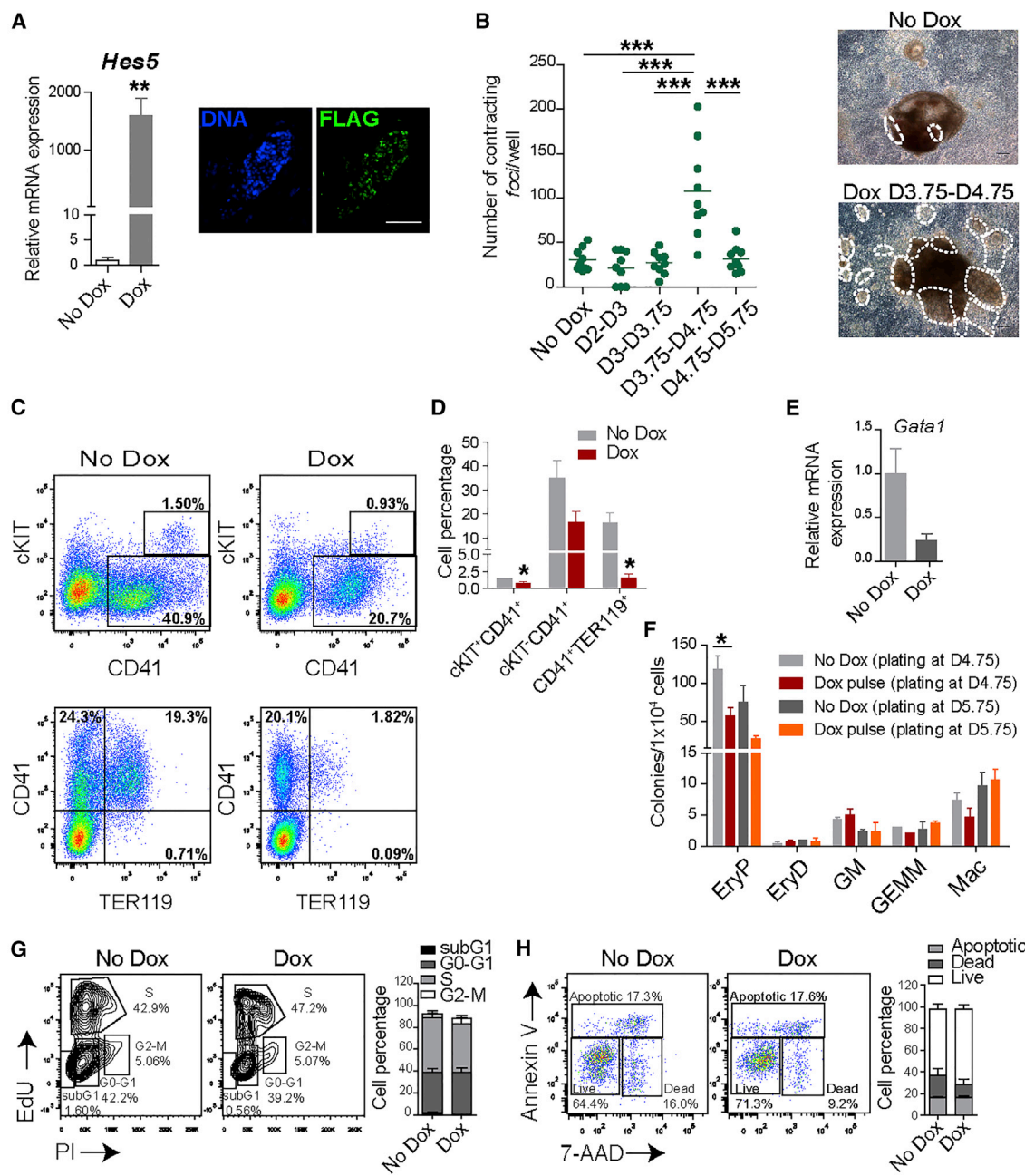


Figure 3. A Pulse of *Hes5* Instructs Preferential Cardiac Over Primitive Erythroid Differentiation in mESC-Derived Mesodermal Cells

(A) *Hes5* mRNA levels and mESC colony expressing FLAG after Dox treatment. Scale bar, 50 μ m.

(B) Quantification of contracting foci per well (three wells per biological triplicate) in non-induced (No Dox) cells and after Dox treatment from D2–D3, D3–D3.75, D3.75–D4.75, or D4.75–D5.75. Dashed white lines (right panel) indicate contracting foci in control and after *Hes5* pulse from D3.75 to D4.75. Scale bar, 100 μ m.

(C and D) Flow-cytometry profile (C) and quantification (D) of hematopoietic markers (cKIT, CD41, and TER119) in control and Dox-treated cells.

(E) Real-time qPCR data for *Gata1* in control and Dox-treated cells.

(F) Quantification of hematopoietic colonies resulting from plating at D4.75 or D5.75 in control and after *Hes5* pulse.

(G) Flow-cytometry profile and quantification of Edu-PI-stained cells in No Dox and Dox conditions.

(H) Flow-cytometry profile and quantification of Annexin V-/7-AAD-stained cells in No Dox and Dox conditions.

Error bars represent mean \pm SEM of three experiments. * p < 0.05, ** p < 0.01, *** p < 0.001. See also Movies S3 and S4.

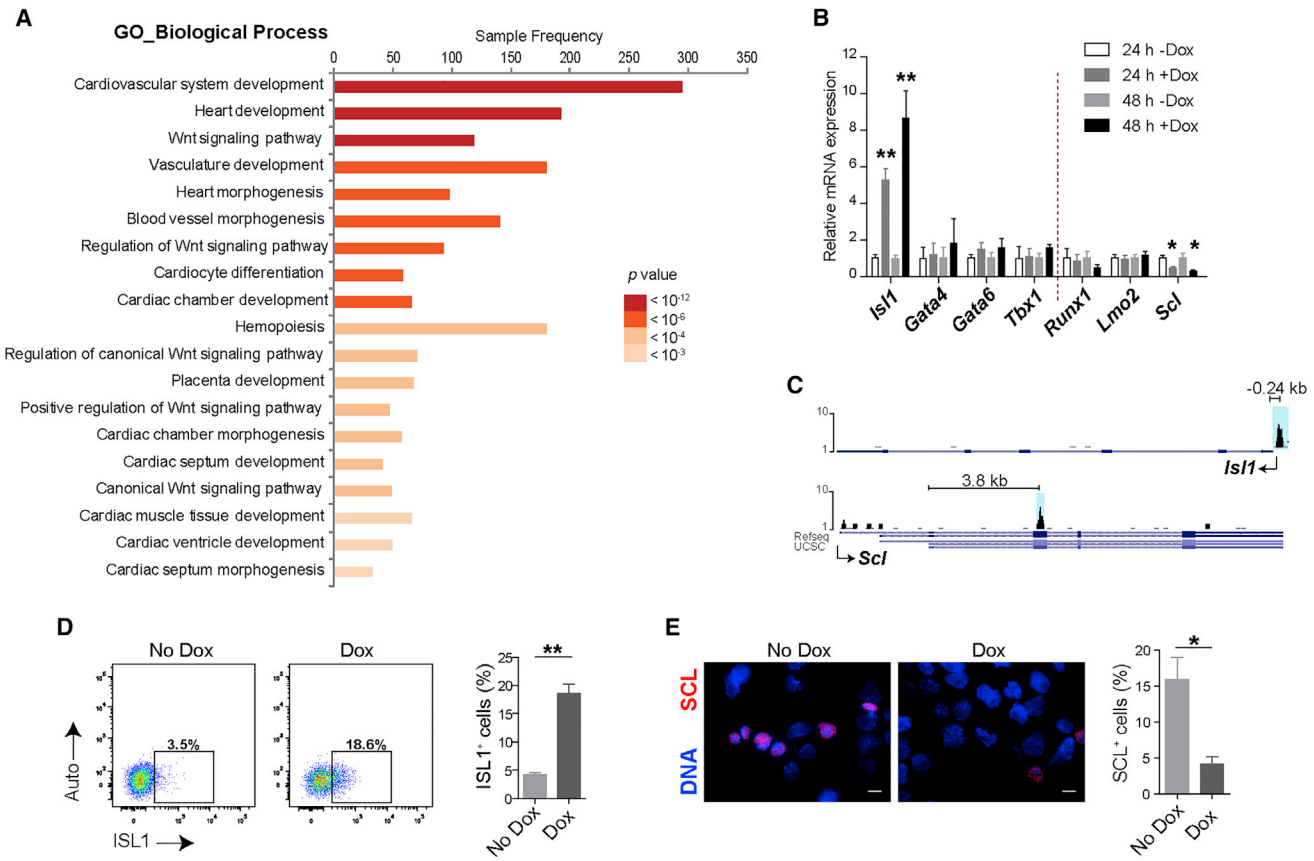


Figure 4. Effect of HES5 in Cardiac and Hematopoietic Gene Expression

- (A) Gene ontology (GO) biological process analysis of HES5 ChIP-seq dataset.
- (B) Real-time qPCR data for cardiac (*Isl1*, *Gata4*, *Gata6*, *Tbx1*) and hematopoietic (*Runx1*, *Lmo2*, *Scl*) genes in control and Dox-treated cells.
- (C) HES5 binding peaks 0.24 kb upstream of the *Isl1* TSS and 3.8 kb downstream of the *Scl* TSS represented in the blue boxes.
- (D) Flow-cytometry profile and quantification of *ISL1*⁺ cells in non-induced and induced cultures. Auto, autofluorescence.
- (E) Immunofluorescence and quantification of *SCL*⁺ cells (>20 fields per biological triplicate) in non-induced and induced cultures. Scale bars, 10 μ m.

Error bars represent mean \pm SEM of three experiments. * $p < 0.05$, ** $p < 0.01$. See also Figure S2; Tables S1 and S2.

includes prevention of DNA binding by lineage-specific bHLH activators (reviewed in Fischer and Gessler, 2007). To gain further mechanistic insight into how HES5 promotes a cardiac fate, we investigated whether HES5 and SCL, also a bHLH protein, form a heterodimeric complex with impaired DNA binding abilities. No protein-protein interaction between HES5 and SCL was found by immunoprecipitation (Figure S2A). To identify genes bound by HES5, we performed chromatin immunoprecipitation combined with DNA sequencing (ChIP-seq) 48 hr after *Hes5* induction at D3.75 (Figures S2B and S2C; Table S1). Using the Panther classification system, cardiovascular and vascular/hematopoietic developmental processes and the Wnt pathway were highly enriched categories (Figure 4A and Table S2). The expression of cardiac (*Isl1*, *Gata4*, *Gata6*, and *Tbx1*) and hematopoietic (*Runx1*,

Lmo2, and *Scl*) genes bound by HES5 according to the ChIP-seq data (Figure S2D) was analyzed. *Isl1* and *Scl* responded significantly to *Hes5* induction, being upregulated (5.3-fold) and downregulated (2.1-fold), respectively, 24 hr after Dox addition, and further increased (8.7-fold) and decreased (3.6-fold), respectively, after 48 hr. The other genes showed no or only moderate alteration in the mRNA levels (Figure 4B). HES5 binding peaks were found 0.24 kb upstream of the *Isl1* transcription start site (TSS) and 3.8 kb downstream of the *Scl* TSS (Figure 4C). Moreover, an increase in the percentage of *ISL1*⁺ cells (4.4-fold) (Figure 4D) and decrease of *SCL*⁺ cells (3.8-fold) (Figure 4E) 48 hr after *Hes5* induction reflected the preferential choice toward cardiac over hematopoietic lineage. Together, these findings show that HES5 binds regulators of vascular/hematopoietic and heart development, including *Scl* and

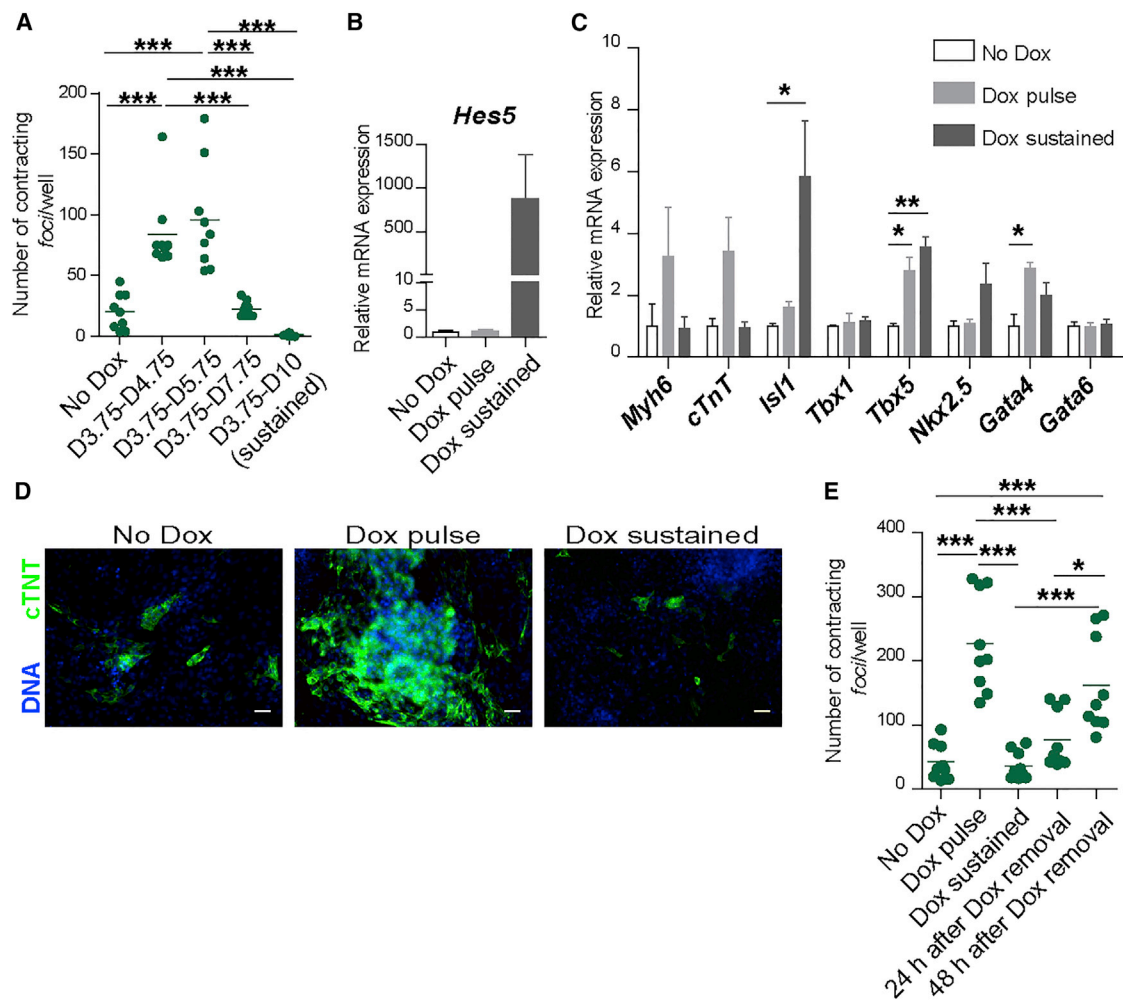


Figure 5. A Dual Role for HES5 in Cardiogenesis

(A) Quantification of contracting foci per well (three wells per biological triplicate) in non-induced cells and after *Hes5* induction from D3.75–D4.75, D3.75–D5.75, D3.75–D7.75, and D3.75–D10 (sustained).

(B) *Hes5* mRNA levels at D10 in non-induced, and after pulse and sustained Dox treatment.

(C) Real-time qPCR data for *Myh6*, *cTnT*, *Isl1*, *Tbx1*, *Tbx5*, *Nkx2.5*, *Gata4*, and *Gata6* in non-induced cells, and after pulse and sustained *Hes5* overexpression.

(D) Immunostaining for cTNT in non-induced cells, and after pulse and sustained *Hes5* overexpression. Scale bars, 50 μm.

(E) Quantification of contracting foci per well (three wells per biological triplicate) after Dox removal.

Error bars represent mean ± SEM of three experiments. *p < 0.05, **p < 0.01, ***p < 0.001.

Isl1, which likely mediate in part the preferential cardiac cell fate decision downstream of HES5.

Sustained *Hes5* Expression after Cardiac Induction Impairs Differentiation to Contracting Cardiomyocytes

Our results showed that a specific pulse of *Hes5* induction from D3.75 to D4.75 enhanced cardiac differentiation (Figure 3B). Moreover, the transient profile of *Hes5* expression in differentiating mESCs (Figures 1A and 1B) and gastrulating embryos (Figure 1C), suggest that after inducing

a cardiac fate *Hes5* downregulation might be required. Thus, we evaluated the effect of increasing periods of Dox treatment, i.e., D3.75–D4.75, D3.75–D5.75, D3.75–D7.75, and D3.75–D10 (sustained), on cardiac differentiation. Activation for 24 and 48 hr significantly enhanced the number of contracting foci, whereas sustained *Hes5* almost abrogated the emergence of contracting foci (Figure 5A). We asked whether a sustained *Hes5* induction blocks differentiation to contracting cardiomyocytes. Expression of structural genes of cardiomyocytes (*Myh6* and *cTnT*) and cardiac progenitor genes (*Isl1*, *Tbx1*, *Tbx5*,



Nkx2.5, *Gata4*, and *Gata6*) was evaluated at D10 in cells subjected to pulse (24 hr) or sustained *Hes5* activation. As expected, *Hes5* was upregulated after sustained Dox, whereas pulse-activated cells showed levels comparable with control levels (Figure 5B). *Tbx5* and *Isl1*, usually associated with first and second heart field progenitors (FHF and SHF), respectively, were significantly upregulated (3.5- and 5.8-fold, respectively) after sustained *Hes5* expression (Figure 5C). *Myh6* and *cTnT* mRNA levels were upregulated (3.2- and 3.4-fold, respectively) (Figure 5C) and cTNT protein detection was more prominent (Figure 5D) in cells subjected to *Hes5* pulse, but were comparable with control levels after sustained induction. To confirm whether sustained *Hes5* activation impairs cardiomyocytic differentiation, we removed Dox after 10 days of treatment. The number of contracting foci at 48 hr after Dox withdrawal was not significantly different from pulse-activated cultures and was significantly increased compared with non-induced (3.8-fold) and sustained Dox treatment (4.4-fold) conditions (Figure 5E). Our results demonstrate that after cardiac specification, *Hes5* withdrawal is required for completing differentiation to contracting cardiomyocytes.

DISCUSSION

Here we established a role for HES5 in instructing a cardiac fate while repressing the hemogenic program in early mesodermal progenitors. In *Hes5*-KD the first hematopoietic wave of primitive erythropoiesis overrides the cardiac potential, whereas a stage-specific *Hes5* overexpression results in enhanced cardiac differentiation. Importantly, we show *Hes5* expression in early mesoderm at the onset of gastrulation, which closely resembles the transient pattern of *Mesp1* (E6.5–E7.0) and correlates with the time cardiac progenitors are specified (Saga et al., 1999). Moreover, the unaltered frequency of cell proliferation and apoptosis after *Hes5* induction further imply an instructive rather than a selective role in primitive mesoderm.

To date, a role for HES5 in cardiac development has not been demonstrated. *Hes5*-null embryos have no apparent cardiovascular phenotype, but to our knowledge studies specifically addressing heart malformations in the mutants have not been performed. Nonetheless, HES5 function may be compensated by another HES/HEY protein, as functional redundancy between members of these families has been shown at later stages of heart morphogenesis (Fischer et al., 2007; Kokubo et al., 2005). For example, *Hey1*, *Hey2*, and *Heyl* play important roles in heart formation but, with exception of *Hey2*-null mice, only the double mutants show cardiac abnormalities (reviewed in Nemir and Pedrazzini, 2008).

Repression of the hematopoietic/erythroid program to ensure cardiac fate determination in mesodermal cells has been previously demonstrated (Caprioli et al., 2011). Our data show that HES5 binds regulators of vascular/hematopoietic and heart development, including *Scl* and *Isl1*, which likely mediate in part preferential cardiac cell fate decision downstream of HES5. Homozygous *Isl1*-null mice have several heart abnormalities, dying by E10.5 (Cai et al., 2003), and *Isl1* overexpression in mESCs enhances specification of cardiac progenitors (Dorn et al., 2015). ISL1 has been referred as an SHF marker; however, the expression in pre-cardiac mesoderm and in the cardiac crescent, as well as the contribution to derivatives of both heart fields, suggest ISL1 to be a pan-cardiac progenitor marker (Brade et al., 2007; Ma et al., 2008; Prall et al., 2007; Yuan and Schoenwolf, 2000). *Scl*-deficient embryos show ectopic cardiogenesis in prospective hemogenic endothelium (Van Handel et al., 2012) and die by E9.5, lacking hematopoiesis in the yolk sac (Robb et al., 1995).

In the embryo brain, HES5 maintains undifferentiated neural stem cells, which are then capable to differentiate after downregulation (Ohtsuka et al., 2001). We demonstrate a similar role in cardiogenesis, since sustained *Hes5* impairs the emergence of contracting colonies, whereas downregulation after cardiac induction allows cardiomyocytic differentiation. These findings further imply a transient role for HES5 during early mesodermal specification to its derivatives, which is corroborated by the pattern of expression we observed in gastrulating embryos. Thus HES5 plays a dual role in cardiogenesis, promoting cardiac fate specification as a pulse, while impairing differentiation to cardiomyocytes when activated in a sustained manner. Our results are in line with previous evidence for an inhibitory effect of Notch in cardiogenesis, which appears to correlate with activation at the level of development and maturation of the cardiac lineage but not upon its induction (Chen et al., 2008; Liu et al., 2014; Rones et al., 2000; Watanabe et al., 2006).

Interestingly, and suggesting a conserved mechanism throughout evolution, *esr9*, a member of the *Hes5*-like subfamily expressed in *Xenopus* (Li et al., 2003), regulates the timing of heart field specification, repressing cardiac differentiation when induced after gastrulation (Miazga and McLaughlin, 2009).

Herein, we identified an important player downstream of NICD1 that sets in motion cardiogenesis and represses hematopoietic commitment in early mesodermal precursors. Notably, the effect of *Hes5* on primitive erythropoiesis is consistent with the required inhibition of Notch signaling for development of this lineage (Cheng et al., 2008), while NOTCH1 is essential for definitive hematopoiesis (Kumano et al., 2003). Furthermore, our data

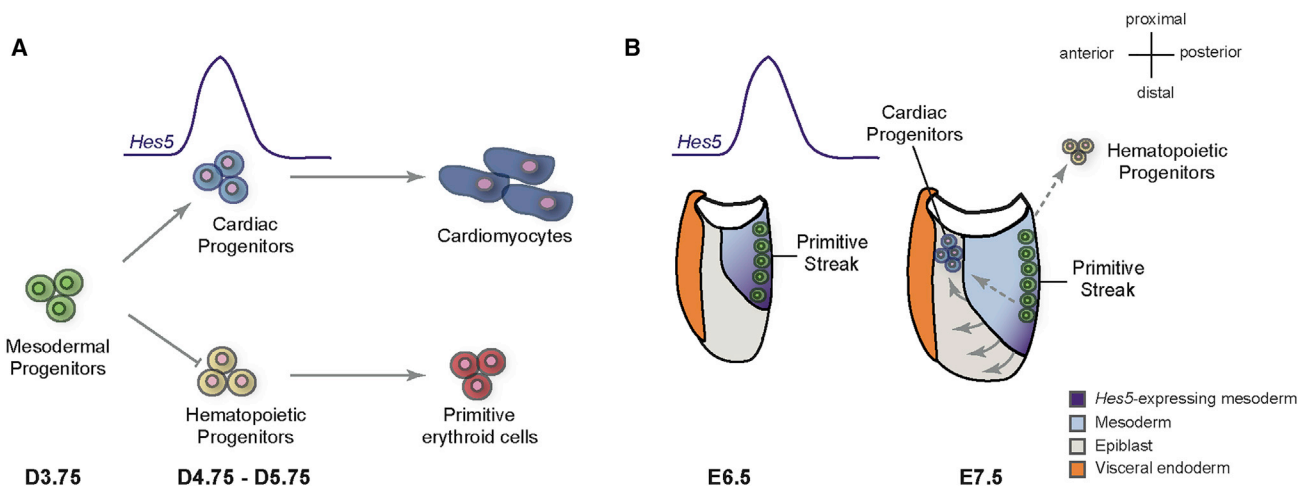


Figure 6. Proposed Model for HES5 Role in Cardiac versus Primitive Erythroid Cell Fate Determination

(A) Transient *Hes5* expression in mESC-derived mesodermal cells from D3.75 to D4.75/D5.75 instructs specification of cardiac fate while repressing primitive erythropoiesis. After induction of cardiac fate, *Hes5* downregulation allows differentiation to contracting cardiomyocytes.

(B) A similar mechanism is likely to take place in the embryo. *Hes5* is expressed in the nascent mesoderm of streak-stage embryos at the time cardiac and hematopoietic progenitors are specified (~E6.5). Around E7.5 cardiac progenitors that left the primitive streak organize to form the cardiac crescent while hematopoietic progenitors have migrated to the yolk sac, coinciding with downregulated *Hes5* expression in the mesoderm.

reinforce the context-specific and time-dependent nature of HES proteins, i.e., not only the timing of induction but also the duration of the signal affects cell fate determination and differentiation.

Hence, we propose a model in which transient HES5 activity in early mesoderm instructs the timing of cardiac fate specification while repressing the first wave of hematopoiesis. Thus in the absence of this signal, commitment to EryP is favored by default. Moreover, after a pulse of *Hes5* instructing a cardiac fate, downregulation is required for emergence of contracting cardiomyocytes (Figure 6A). Our observation of *Hes5* transient expression in early embryo mesoderm at the time cardiac and hematopoietic progenitors are specified strongly indicates that a similar mechanism is likely to occur during embryogenesis (Figure 6B). Although challenging given the risk for the successful progression of embryo development, further *in vivo* analyses, including lineage tracing of the progeny derived from the transient *Hes5*-expressing nascent mesoderm, will be required to ultimately demonstrate a role in specifying cardiac fate in the embryo.

In conclusion, this study establishes a role for HES5 in cardiogenesis, contributing further insight into the complex signaling that regulates cardiac fate determination and paving the way for future mechanistic studies aimed at the validation and comprehension of how HES5 imparts heart formation in the developing embryo.

EXPERIMENTAL PROCEDURES

mESC Lines

The AinV/Bry-GFP/NICD1 and AinV/Bry-GFP mESC lines (Cheng et al., 2008) were a kind gift from Dr. Gordon M. Keller and Dr. Valerie Gouon-Evans.

mESC Culture and Differentiation

mESCs were maintained in the absence of feeders on 0.1% gelatin-coated (Sigma-Aldrich) plates in the presence of 15% fetal bovine serum (FBS) (BenchMark, catalog lot no. A00D05C) and 1,000 U/mL leukemia inhibitory factor (Esgro, Millipore). Differentiation to mesoderm was induced as previously described (Gadue et al., 2006; Kattman et al., 2011) with few modifications. In brief, mESCs were plated at 1–2 × 10⁵ cells/mL in serum-free differentiation medium in ultra-low-attachment 6-well plates (Corning) for 48 hr to allow formation of embryoid bodies (EBs). After this period EBs were dissociated using TrypLE Express (Gibco, Life Technologies) and plated at 1.5–4 × 10⁵ cells/mL in the presence of 5 ng/mL human vascular endothelial growth factor, 25 ng/mL human activin A, and 1 ng/mL human bone morphogenetic protein 4 (all from R&D Systems) for 42 hr. For cardiac differentiation, D3.75 cells were dissociated and reaggregated at 2 × 10⁵ cells/mL in StemPro-34+StemPro-Nutrient Supplement (Gibco, Life Technologies) medium with supplements in ultra-low-attachment 24-well plates (Corning). After 24 hr the aggregates were replated on gelatin-coated 24-well plates as previously described (Chen et al., 2008). Doxycycline (Dox) (1 µg/mL; Sigma-Aldrich) was added to the medium at indicated time points. For CFU assays, D3.75 cells were plated in StemPro-34 medium with supplements for 24 or



48 hr in the presence of Dox when appropriate. Cells were dissociated with TrypLE Express and plated in a methylcellulose-based medium containing hematopoietic cytokines (MethoCult GF M3434, STEMCELL Technologies) at 1.25×10^4 cells/mL. Hematopoietic colonies were counted after 5 days to determine EryP and 8 days to determine EryD, GM, GEMM, and Mac colonies. Detailed media compositions are available in [Supplemental Experimental Procedures](#).

shRNA Design

shRNA sequences were obtained from The RNAi Consortium library database. shRNA oligos were synthesized by Integrated DNA Technologies, annealed, and cloned into AgeI/EcoRI sites of the lentiviral-based shRNA expression vector pLKO.1 (Addgene) ([Moffat et al., 2006](#)) according to the supplier's protocol. shRNA constructs were confirmed by sequencing and are listed in [Table S3](#).

Lentivirus Production and mESC Transduction

Lentiviral-based shRNA vectors and pCMV-dR8.2 (packaging) and pCMV-VSVG (envelope) plasmids were co-transfected into HEK293T cells using the calcium phosphate method described in detail in [Supplemental Experimental Procedures](#). Viral supernatants were harvested after 36, 48, and 72 hr, filtered (0.45 μ m), and concentrated with Amicon ultra-centrifugal filter units (Millipore). mESCs were incubated overnight with virus in medium supplemented with polybrene (8 μ g/mL, Sigma-Aldrich) and cultured in fresh medium for 4 days. After this period, cells were cultured in medium supplemented with 5 μ g/mL blasticidin for an additional 4 days. For *Hes5* overexpression Ainv/Bry-GFP mESC were infected with a lentiviral pTRE-IRES-Bsd^R vector expressing FLAG-tagged *Hes5* under the control of a tetracycline response element promoter. After blasticidin selection and single-cell sorting, colonies were screened for FLAG expression after Dox treatment.

Gene Expression Analysis

RNA was extracted using TRIzol reagent (Invitrogen) according to the manufacturer's instructions, and cDNA was synthesized using PrimeScript RT reagent kit (Takara Bio). Real-time qPCR was performed using iQ Sybr Green Supermix (Bio-Rad) and gene-specific primers ([Table S4](#)). Reactions were carried out in triplicate on the iCycler iQ5 Real-Time PCR system (Bio-Rad). Relative gene expression was normalized to glyceraldehyde-3-phosphate dehydrogenase (*Gapdh*) expression.

Flow Cytometry

Cells were incubated with phycoerythrin (PE)-conjugated anti-FLK1 (Avas 12 α 1, BD Biosciences) and anti-TER119 (TER-119, Immunotools); allophycocyanin-conjugated anti-PDGFR α /CD140a (AP5, BioLegend), anti-cKIT/CD117 (ACK2, eBioscience), and anti-CD144/VECAD (eBioBV13, eBioscience); and PE-Cyanine7-conjugated anti-CD41 (MWReg30, eBioscience) and anti-CD45 (30-F11, eBioscience) at 1:100 dilution at 4°C for 30 min in PBS containing 3% FBS. All of the antibody clones are commonly used and proven in the field ([Chan et al., 2013; Haas et al., 2012; Pereira et al., 2016](#)); gating was determined using unstained controls. For ISL1 detection, the FOXP3/Transcription Factor Staining

Buffer Set (eBioscience) was used following the manufacturer's instructions. In brief, cells were fixed and permeabilized in the fixation/permeabilization solution for 45 min at room temperature. Cells were washed in permeabilization buffer and incubated with PE-conjugated anti-ISL1 (Q11-465, BD Biosciences) at 1:100 dilution for 60 min at room temperature. PE-conjugated anti-mouse immunoglobulin G antibody was used as control. Flow-cytometry acquisition was performed using FACSCanto II (BD Biosciences) and analyzed using FlowJo software. For cell sorting, cells were resuspended in PBS containing 2% FBS, 25 mM HEPES, and 1 mM EDTA, and sorted using Mo-Flo (DakoCytomation) or FACS Aria (BD Biosciences) cell sorters.

Cell Proliferation and Cell Apoptosis Analyses

Cell proliferation was assessed using the Click-iT Plus EdU cell proliferation kit (Molecular Probes). Cells were incubated with 10 μ M 5-ethynyl-2'-deoxyuridine (EdU) for 5 hr, dissociated with TrypLE Express, and fixed with ice-cold 70% ethanol for 30 min at 4°C. Next, samples were washed with 0.1% Tween 20 and incubated for 30 min at room temperature with Click-iT Plus reaction cocktail. After washing in 0.1% Tween 20, cells were incubated with 50 μ g/mL propidium iodide and 10 μ g/mL RNase for 30 min before acquisition. Apoptosis was assessed using the Annexin V detection kit (eBioscience) according to the manufacturer's protocol. In brief, cells were gently dissociated with StemPro Accutase Cell Dissociation Reagent (Gibco, Life Technologies) for 5 min, and washed in PBS and then in Binding Buffer provided by the kit. V450-conjugated Annexin V was incubated at 1:20 dilution for 15 min at room temperature. After washing in Binding Buffer, samples were incubated with 7-aminoactinomycin D (7-AAD) viability staining solution. Flow-cytometry acquisition was performed using FACSCanto II (BD Biosciences) and analyzed using FlowJo software.

Immunofluorescence

For FLAG and cTNT detection, cells were fixed with 4% paraformaldehyde (PFA) for 20 min and permeabilized with 0.2% Triton X-100 in PBS for 5 min. After blocking in PBS containing 4% FBS and 1% BSA for 60 min, samples were incubated with mouse anti-FLAG (M2, Sigma-Aldrich) at 1:100 dilution or mouse anti-cardiac troponin T (13-11, NeoMarkers/Thermo Scientific) at 1:500 dilution for 120 min, followed by anti-mouse 488 for 60 min. For SCL staining, cells were dissociated, cytospun into slides, and fixed with cold methanol for 2 min. After permeabilization with 1% Triton X-100 in PBS for 5 min, blocking was performed using 4% FBS and 1% BSA in PBS for 60 min. Incubation with goat anti-SCL (C21, Santa Cruz Biotechnology, sc-12984X) at 1:10,000 dilution was carried out for 90 min and followed by incubation with secondary antibody donkey anti-goat 568 for 45 min. For nuclei staining, samples were incubated with DAPI at 0.5 μ g/mL or mounted in Vectashield with DAPI (Vector Laboratories). Images were acquired using Leica DMI4000 (Leica) or Axiovert 200 (Zeiss) microscopes.

Whole-Mount *In Situ* Hybridization

C57BL/6 (Charles River) pregnant females and embryos were used in this study. All animal work was approved by the i3S Animal



Ethics Committee and by the Direcção Geral de Veterinária (permit 022793), and is in conformity with the Directive 2010/63/EU of the European Parliament. Humane end points were followed in accordance to the OECD Guidance Document on the Recognition, Assessment, and Use of Clinical Signs as Humane End Points for Experimental Animals Used in Safety Evaluation. The day of the vaginal plug was designated embryonic day (E) 0.5(E0.5). Embryos were staged according to the dissection time and morphology as previously described (Downs and Davies, 1993). E6.5–E9.5 embryos were fixed overnight at 4°C in 4% PFA at pH 7.4 and whole-mount *in situ* hybridization was performed as previously described (Henrique et al., 1995). In brief, embryos were dehydrated in a graded series of methanol, treated with 10 µg/mL Proteinase K (Sigma-Aldrich), and post-fixed for 20 min in 4% PFA and 0.1% glutaraldehyde. Embryos were incubated with digoxigenin-labeled *Hes5* antisense probe (a gift from Dr. Domingos Henrique) overnight at 65°C and with anti-digoxigenin antibody at 1:2,000 dilution (Roche) overnight at 4°C. Detection was performed using NBT/BCIP (Roche). Photographs were acquired using an Olympus SZX16 stereomicroscope. For cryosectioning, embryos were dehydrated in a sucrose gradient (4% followed by 15%), embedded in 7.5% gelatin, and frozen. Tissue sections (12 µm) were obtained using a Leica cryostat, mounted in Fluoromount (Sigma-Aldrich), and photographed using an Axiovert 200 (Zeiss) microscope.

ChIP-Seq Sample Preparation and Analysis

Sample preparation and analysis were performed as previously described (Waghray et al., 2015). Procedures are described in detail in [Supplemental Experimental Procedures](#).

Statistical Analysis

Pooled data from biological replicates is presented as mean ± SEM. Statistical significance was determined by unpaired two-tailed t test (comparison between two groups) or ANOVA with post hoc Tukey's test (comparison between three or more groups) using GraphPad Prism. $p < 0.05$ was considered statistically significant.

ACCESSION NUMBERS

ChIP-seq data are deposited in NCBI-GEO database under accession number GEO: GSE64540.

SUPPLEMENTAL INFORMATION

Supplemental Information includes Supplemental Experimental Procedures, two figures, four tables, and four movies and can be found with this article online at <http://dx.doi.org/10.1016/j.stemcr.2017.05.025>.

AUTHOR CONTRIBUTIONS

A.G.F., A.W., F.S.-S., T.P.R., and D.-F.L. conceived and performed experiments and analyzed the data; C.-F.P. and D.S.N. conceived and provided critical suggestions; A.G.F. wrote the manuscript; A.W., F.S.-S., T.P.R., D.F.-L., C.-F.P., and D.S.N. reviewed the manuscript; I.R.L. and P.P.-Ó. conceived and supervised the work, acquired funding, and reviewed the manuscript.

ACKNOWLEDGMENTS

We thank Dr. G. Keller and Dr. V. Gouon-Evans for the mESC lines, Dr. D. Henrique for the *Hes5* probe, members of I.R.L./Moore and P.P.-Ó. laboratories for useful discussions, and Dr. V. Taylor and Dr. B. Bruneau for technical help. We thank hESC/hiPSC, Genomics and Flow Cytometry shared resource facilities at Icahn School of Medicine at Mount Sinai and i3S Cell Culture and Genotyping Service, Animal Facility and Advanced Flow Cytometry Unit. Research was funded by NIH (5R01GM078465) and the Empire State Stem Cell Fund through New York State Department of Health (NYSYSTEM: C024176) to I.R.L.; by European Structural and Investment Funds (ESIF), under Lisbon Portugal Regional Operational Programme and National Funds through Foundation for Science and Technology (FCT) under project POCI-01-0145-FEDER-016385 to P.P.-Ó. A.G.F. and T.P.R. were supported by FCT (SFRH/BD/64715/2009 and SFRH/BPD/80588/2011, respectively); D.-F.L. by NIH Pathway to Independence Award (K99CA181496); and C.-F.P. by Charles H. Revson Senior Fellowship in Biomedical Science (New York) and FCT investigator IF/00646/2015. P.P.-Ó. was recipient of an invited scientist grant by Institut Pasteur, Paris, France. The authors are indebted to Dr. A. Cumano, Dr. K. Moore, and Dr. G. Keller for critical revision of the manuscript.

Received: May 9, 2017

Revised: May 18, 2017

Accepted: May 19, 2017

Published: June 22, 2017

REFERENCES

- Brade, T., Gessert, S., Kuhl, M., and Pandur, P. (2007). The amphibian second heart field: *Xenopus* *islet-1* is required for cardiovascular development. *Dev. Biol.* **311**, 297–310.
- Cai, C.L., Liang, X., Shi, Y., Chu, P.H., Pfaff, S.L., Chen, J., and Evans, S. (2003). *Isl1* identifies a cardiac progenitor population that proliferates prior to differentiation and contributes a majority of cells to the heart. *Dev. Cell* **5**, 877–889.
- Caprioli, A., Koyano-Nakagawa, N., Iacovino, M., Shi, X., Ferdous, A., Harvey, R.P., Olson, E.N., Kyba, M., and Garry, D.J. (2011). *Nkx2-5* represses *Gata1* gene expression and modulates the cellular fate of cardiac progenitors during embryogenesis. *Circulation* **123**, 1633–1641.
- Chan, S.S., Shi, X., Toyama, A., Arpke, R.W., Dandapat, A., Iacovino, M., Kang, J., Le, G., Hagen, H.R., Garry, D.J., et al. (2013). *Mesp1* patterns mesoderm into cardiac, hematopoietic, or skeletal myogenic progenitors in a context-dependent manner. *Cell Stem Cell* **12**, 587–601.
- Chen, V.C., Stull, R., Joo, D., Cheng, X., and Keller, G. (2008). Notch signaling respecifies the hemangioblast to a cardiac fate. *Nat. Biotechnol.* **26**, 1169–1178.
- Cheng, X., Huber, T.L., Chen, V.C., Gadue, P., and Keller, G.M. (2008). Numb mediates the interaction between Wnt and Notch to modulate primitive erythropoietic specification from the hemangioblast. *Development* **135**, 3447–3458.
- Del Monte, G., Grego-Bessa, J., Gonzalez-Rajal, A., Bolos, V., and De La Pompa, J.L. (2007). Monitoring Notch1 activity in



- development: evidence for a feedback regulatory loop. *Dev. Dyn.* **236**, 2594–2614.
- Dorn, T., Goedel, A., Lam, J.T., Haas, J., Tian, Q., Herrmann, F., Bundschu, K., Dobreva, G., Schiemann, M., Dirschniger, R., et al. (2015). Direct *nkx2-5* transcriptional repression of *isl1* controls cardiomyocyte subtype identity. *Stem Cells* **33**, 1113–1129.
- Downs, K.M., and Davies, T. (1993). Staging of gastrulating mouse embryos by morphological landmarks in the dissecting microscope. *Development* **118**, 1255–1266.
- Fischer, A., and Gessler, M. (2007). Delta-Notch—and then? Protein interactions and proposed modes of repression by Hes and Hey bHLH factors. *Nucleic Acids Res.* **35**, 4583–4596.
- Fischer, A., Steidl, C., Wagner, T.U., Lang, E., Jakob, P.M., Friedl, P., Knobeloch, K.P., and Gessler, M. (2007). Combined loss of Hey1 and HeyL causes congenital heart defects because of impaired epithelial to mesenchymal transition. *Circ. Res.* **100**, 856–863.
- Freire, A.G., Resende, T.P., and Pinto-do, O.P. (2014). Building and repairing the heart: what can we learn from embryonic development? *Biomed. Res. Int.* **2014**, 679168.
- Gadue, P., Huber, T.L., Paddison, P.J., and Keller, G.M. (2006). Wnt and TGF-beta signaling are required for the induction of an *in vitro* model of primitive streak formation using embryonic stem cells. *Proc. Natl. Acad. Sci. USA* **103**, 16806–16811.
- Haas, J.D., Ravens, S., Duber, S., Sandrock, I., Oberdorfer, L., Kashani, E., Chennupati, V., Fohse, L., Naumann, R., Weiss, S., et al. (2012). Development of interleukin-17-producing gamma-delta T cells is restricted to a functional embryonic wave. *Immunity* **37**, 48–59.
- Henrique, D., Adam, J., Myat, A., Chitnis, A., Lewis, J., and Ish-Horowicz, D. (1995). Expression of a Delta homologue in prospective neurons in the chick. *Nature* **375**, 787–790.
- High, F.A., and Epstein, J.A. (2008). The multifaceted role of Notch in cardiac development and disease. *Nat. Rev. Genet.* **9**, 49–61.
- Kageyama, R., Ohtsuka, T., and Kobayashi, T. (2007). The Hes gene family: repressors and oscillators that orchestrate embryogenesis. *Development* **134**, 1243–1251.
- Kataoka, H., Hayashi, M., Nakagawa, R., Tanaka, Y., Izumi, N., Nishikawa, S., Jakt, M.L., and Tarui, H. (2011). Etv2/ER71 induces vascular mesoderm from Flk1+PDGFRalpha+ primitive mesoderm. *Blood* **118**, 6975–6986.
- Kattman, S.J., Witty, A.D., Gagliardi, M., Dubois, N.C., Niapour, M., Hotta, A., Ellis, J., and Keller, G. (2011). Stage-specific optimization of activin/nodal and BMP signaling promotes cardiac differentiation of mouse and human pluripotent stem cell lines. *Cell Stem Cell* **8**, 228–240.
- Kokubo, H., Miyagawa-Tomita, S., Nakazawa, M., Saga, Y., and Johnson, R.L. (2005). Mouse *hesr1* and *hesr2* genes are redundantly required to mediate Notch signaling in the developing cardiovascular system. *Dev. Biol.* **278**, 301–309.
- Kumano, K., Chiba, S., Kunisato, A., Sata, M., Saito, T., Nakagami-Yamaguchi, E., Yamaguchi, T., Masuda, S., Shimizu, K., Takahashi, T., et al. (2003). Notch1 but not Notch2 is essential for generating hematopoietic stem cells from endothelial cells. *Immunity* **18**, 699–711.
- Li, Y., Fenger, U., Niehrs, C., and Pollet, N. (2003). Cyclic expression of *esr9* gene in *Xenopus* presomitic mesoderm. *Differentiation* **71**, 83–89.
- Liu, Y., Li, P., Liu, K., He, Q., Han, S., Sun, X., Li, T., and Shen, L. (2014). Timely inhibition of Notch signaling by DAPT promotes cardiac differentiation of murine pluripotent stem cells. *PLoS One* **9**, e109588.
- Ma, Q., Zhou, B., and Pu, W.T. (2008). Reassessment of *Isl1* and *Nkx2-5* cardiac fate maps using a *Gata4*-based reporter of Cre activity. *Dev. Biol.* **323**, 98–104.
- Miazga, C.M., and McLaughlin, K.A. (2009). Coordinating the timing of cardiac precursor development during gastrulation: a new role for Notch signaling. *Dev. Biol.* **333**, 285–296.
- Moffat, J., Grueneberg, D.A., Yang, X., Kim, S.Y., Kloepfer, A.M., Hinkle, G., Piqani, B., Eisenhaure, T.M., Luo, B., Grenier, J.K., et al. (2006). A lentiviral RNAi library for human and mouse genes applied to an arrayed viral high-content screen. *Cell* **124**, 1283–1298.
- Murry, C.E., and Keller, G. (2008). Differentiation of embryonic stem cells to clinically relevant populations: lessons from embryonic development. *Cell* **132**, 661–680.
- Nemir, M., and Pedrazzini, T. (2008). Functional role of Notch signaling in the developing and postnatal heart. *J. Mol. Cell Cardiol* **45**, 495–504.
- Ohtsuka, T., Sakamoto, M., Guillemot, F., and Kageyama, R. (2001). Roles of the basic helix-loop-helix genes *Hes1* and *Hes5* in expansion of neural stem cells of the developing brain. *J. Biol. Chem.* **276**, 30467–30474.
- Parameswaran, M., and Tam, P.P. (1995). Regionalisation of cell fate and morphogenetic movement of the mesoderm during mouse gastrulation. *Dev. Genet.* **17**, 16–28.
- Pereira, C.F., Chang, B., Gomes, A., Bernitz, J., Papatsenko, D., Niu, X., Swiers, G., Azzoni, E., de Bruijn, M.F., Schaniel, C., et al. (2016). Hematopoietic reprogramming *in vitro* informs *in vivo* identification of hemogenic precursors to definitive hematopoietic stem cells. *Dev. Cell* **36**, 525–539.
- Prall, O.W., Menon, M.K., Solloway, M.J., Watanabe, Y., Zaffran, S., Bajolle, F., Biben, C., McBride, J.J., Robertson, B.R., Chaulet, H., et al. (2007). An *Nkx2-5/Bmp2/Smad1* negative feedback loop controls heart progenitor specification and proliferation. *Cell* **128**, 947–959.
- Robb, L., Lyons, I., Li, R., Hartley, L., Kontgen, F., Harvey, R.P., Metcalf, D., and Begley, C.G. (1995). Absence of yolk sac hematopoiesis from mice with a targeted disruption of the *scl* gene. *Proc. Natl. Acad. Sci. USA* **92**, 7075–7079.
- Rones, M.S., McLaughlin, K.A., Raffin, M., and Mercola, M. (2000). Serrate and Notch specify cell fates in the heart field by suppressing cardiomyogenesis. *Development* **127**, 3865–3876.
- Saga, Y., Miyagawa-Tomita, S., Takagi, A., Kitajima, S., Miyazaki, J., and Inoue, T. (1999). MesP1 is expressed in the heart precursor cells and required for the formation of a single heart tube. *Development* **126**, 3437–3447.
- Tavian, M., and Peault, B. (2005). Embryonic development of the human hematopoietic system. *Int. J. Dev. Biol.* **49**, 243–250.



- Van Handel, B., Montel-Hagen, A., Sasidharan, R., Nakano, H., Ferrari, R., Boogerd, C.J., Schredelseker, J., Wang, Y., Hunter, S., Org, T., et al. (2012). Scl represses cardiomyogenesis in prospective hemogenic endothelium and endocardium. *Cell* **150**, 590–605.
- Waghray, A., Saiz, N., Jayaprakash, A.D., Freire, A.G., Papatsenko, D., Pereira, C.F., Lee, D.F., Brosh, R., Chang, B., Darr, H., et al. (2015). Tbx3 controls Dppa3 levels and exit from pluripotency toward mesoderm. *Stem Cell Rep.* **5**, 97–110.
- Watanabe, Y., Kokubo, H., Miyagawa-Tomita, S., Endo, M., Igarashi, K., Aisaki, K., Kanno, J., and Saga, Y. (2006). Activation of Notch1 signaling in cardiogenic mesoderm induces abnormal heart morphogenesis in mouse. *Development* **133**, 1625–1634.
- Yuan, S., and Schoenwolf, G.C. (2000). Islet-1 marks the early heart rudiments and is asymmetrically expressed during early rotation of the foregut in the chick embryo. *Anat. Rec. Anat. Rec.* **260**, 204–207.